Environmental Science and Pollution Research (2018) 25:14868–14881
https://doi.org/10.1007/s11356-018-1713-z

RESEARCH ARTICLE

Observation of optical properties and sources of aerosols at Buddha's birthplace, Lumbini, Nepal: environmental implications

Dipesh Rupakheti[1,2,3] · Shichang Kang[2,3,4] · Maheswar Rupakheti[5,6] · Zhiyuan Cong[1,4] · Lekhendra Tripathee[3] · Arnico K. Panday[7] · Brent N. Holben[8]

Received: 23 August 2017 / Accepted: 8 March 2018 / Published online: 15 March 2018

Abstract

For the first time, aerosol optical properties are measured over Lumbini, Nepal, with CIMEL sunphotometer of the Aerosol Robotic Network (AERONET) program. Lumbini is a sacred place as the birthplace of Lord Buddha, and thus a UNESCO world heritage site, located near the northern edge of the central Indo-Gangetic Plains (IGP) and before the Himalayan foothills (and Himalayas) to its north. Average aerosol optical depth (AOD) is found to be 0.64 ± 0.38 (0.06–3.28) over the sampling period (January 2013–December 2014), with the highest seasonal AOD during the post-monsoon season (0.72 ± 0.44). More than 80% of the daily averaged AOD values, during the monitoring period, are above 0.3, indicating polluted conditions in the region. The levels of aerosol load observed over Lumbini are comparable to those observed at several heavily polluted sites in the IGP. Based on the relationship between AOD and Ångstrom exponent (α), anthropogenic, biomass burning, and mixed aerosols are found to be the most prevalent aerosol types. The aerosol volume-size distribution is bi-modal during all four seasons with modes centered at 0.1–0.3 and 3–4 μm. For both fine and coarse modes, the highest volumetric concentration of ~ 0.08 μm^{-3} μm^{-2} is observed during the post-monsoon and pre-monsoon seasons. As revealed by the single-scattering albedo (SSA), asymmetry parameter (AP), and refractive index (RI) analyses, aerosol loading over Lumbini is dominated by absorbing, urban-industrial, and biomass burning aerosols.

Keywords Aerosol optical depth · Ångstrom exponent · Indo-Gangetic Plain · Lumbini · Himalayas · Nepal

Introduction

Atmospheric aerosols of both natural and anthropogenic origins have important influences on the radiation balance of the earth through multiple ways: directly by affecting the scattering and absorption of solar radiation, indirectly by altering cloud microphysics and lifetime, and semi-directly by affecting cloud formation or evaporation (Kaufman et al. 2002; Ramanathan and Carmichael 2008). However, due to inadequate knowledge about the physical, optical, and

Responsible editor: Gerhard Lammel

✉ Dipesh Rupakheti
drupakheti2@gmail.com

✉ Shichang Kang
shichang.kang@lzb.ac.cn

[1] Key Laboratory of Tibetan Environment Changes and Land Surface Processes, Institute of Tibetan Plateau Research, Chinese Academy of Sciences, Beijing 100101, China

[2] University of Chinese Academy of Sciences, Beijing 100049, China

[3] State Key Laboratory of Cryospheric Science, Northwest Institute of Eco-Environment and Resources, Chinese Academy of Sciences, Lanzhou 730000, China

[4] Center for Excellence in Tibetan Plateau Earth Sciences, Chinese Academy of Sciences, Beijing 100101, China

[5] Institute for Advanced Sustainability Studies (IASS), Potsdam, Germany

[6] Himalayan Sustainability Institute (HIMSI), Kathmandu, Nepal

[7] International Centre for Integrated Mountain Development (ICIMOD), Lalitpur, Nepal

[8] NASA Goddard Space Flight Center, Greenbelt, MD, USA

chemical properties of anthropogenic aerosols (Kaufman et al. 2002), a large source of uncertainty exists in understanding the role of aerosols in the climate system (Stocker et al. 2013). Complex aerosol optical and microphysical properties over a wide range of both temporal and spatial scales are major reasons why scientific understanding of aerosols is still limited (Srivastava et al. 2011), particularly in downwind regions of highly polluted regions of Asia. Past studies have already shown that the anthropogenic aerosols can alter regional climate, hydrological cycle, clouds, and precipitation (Ramanathan et al. 2001; Rosenfeld 2000). The major challenge in the current climatic study is to characterize the variation of concentration, composition, and size of aerosols at regional scale with sufficiently high temporal and spatial resolution (Alam et al. 2014), which requires approaches that combine measurements and atmospheric modeling.

The Indo-Gangetic Plain (IGP) region is one of the most populated, polluted, and heavily aerosol-laden regions of the world, which also affects downwind regions in the foothills of the Himalayas, Himalayas, and the Tibetan Plateau (Ganguly et al. 2006; Gautam et al. 2011; Lüthi et al. 2015; Srivastava et al. 2011). The IGP is often covered by recurrent thick layers of regional air pollution blanket during the dry season every year, commonly referred to as Atmospheric Brown Clouds (ABC) (Ramanathan and Crutzen 2003). Major sources of air pollution in the IGP are biomass burning (Habib et al. 2006), vehicles, and industries (Ram and Sarin 2011, 2015), as well as desert dust during the pre-monsoon season (Srivastava et al. 2012b). Due to insufficient spatial and temporal measurements of aerosol properties over the region to date, it is important to work towards improvements in aerosol characterization over the IGP and the surrounding regions, especially the relatively poorly sampled Himalayan foothills and mountain regions (Srivastava et al. 2011). Although satellite observations and atmospheric simulations with chemistry transport models have been used for studying the spatial and temporal variation of aerosol properties over a wide area in the IGP (Adhikary et al. 2007; Bibi et al. 2015; Gautam et al. 2009; Mehta 2015), ground-based observations are essential to validate satellite measurements and also provide observational inputs to atmospheric simulation models. Moreover, the satellite aerosol products, such as from the Moderate Resolution Imaging Spectroradiometer (MODIS), are subject to higher uncertainties compared to the ground-based AOD measurements during the dust loading season in South Asia (Tripathi et al. 2005). Even though the ground-based aerosol remote sensing has lower resolution in terms of spatial coverage, we can still obtain reliable and continuous data on aerosol optical properties over particular regionally representative locations (Dubovik et al. 2002). Past studies on aerosol optical properties from both satellite and ground-based measurements have been particularly limited over Nepal, which is characterized by complex mountainous topography and several sensitive ecosystems and landscapes of regional and global significance such as mountain glaciers. However, no study with at least whole year sampling has been conducted on measurements of aerosol loading in the Nepali IGP region until the AERONET site was set up in Lumbini in December 2012. Some past studies pertaining to aerosol optical properties conducted in Nepal have been focused on a high altitude station near the base camp of Mt. Everest (Gobbi et al. 2010; Marcq et al. 2010) or mid-hill sites (Shrestha et al. 2010; Xu et al. 2014). There was a past study (Gautam et al. 2011) which reported short-term aerosol optical properties (ca. 2 weeks to 2 months at each site) at three sites in the foothills of Himalayas in Nepal. The southern plains of Nepal are not only food basket to Nepal but they are also home to several national parks and wildlife reserves, a world heritage site, and historical and archeological sites such as Lumbini.

In this work, variations of aerosol optical properties, mainly the aerosol optical depth (AOD) and the Ångstrom exponent (α), have been analyzed for the period from January 2013 to December 2014 at Lumbini. We conducted source characterization of the aerosols based on the relationship between AOD and α. Similarly, the volume-size distribution and optical properties, including single-scattering albedo, asymmetry parameter, and refractive index of the aerosols for different seasons have also been investigated. Finally, the Hybrid Single-Particle Lagrangian Integrated Trajectory Model (HYSPLIT) has been employed to gain insights into the potential origins of the air masses and consequently sources of air pollution in Lumbini. We believe this work will serve as an important reference because of the unique location in northern IGP, juxtaposed between highly polluted IGP to its south and relatively cleaner foothills of the central Himalaya and the Himalayan-Tibetan region to its north. There is a significant deficit in observational data on (and thus understanding of) the aerosol optical properties in the regions north of the IGP.

Site description and experimental setup

Study area

As a part of the *Sustainable Atmosphere for the Kathmandu Valley-Atmospheric Brown Clouds* (SusKat-ABC) international air pollution measurement campaign conducted in Nepal in 2013, a regional atmospheric measurement site was set up (LIRI, 27.49° N, 83.28° E, 110 m a.s.l.) in Lumbini (Rupandehi District) in southern lowland Nepal (Fig. 1). Based on physiographical and climatic conditions, the region can be classified as a sub-tropical one with annual precipitation of about 1500 mm (Sigdel and Ma 2015). Major sources of nearby air pollution sources include industries (mainly cement factories and brick kilns) and biomass burning for cooking activities and agro-residue burning during two

Fig. 1 Map of Nepal showing the location of Lumbini (black dot) (obtained from National Geographic, http://www.nationalgeographic.com/). The sunphotometer used for this study is shown in the inset

harvesting seasons (rice: November–December and wheat: March–April). Lumbini is also strongly affected by the transport of air pollutants, emitted from various sources in India and beyond, across the India-Nepal border, which is only 8 km to the south of the site. More detailed description of the sampling site has already been provided elsewhere (Rupakheti et al. 2017).

Instrumentation

The NASA Aerosol Robotic Network (AERONET, http://aeronet.gsfc.nasa.gov/) project deployed a CIMEL sun/sky radiometer as an important contribution to the SusKat measurement campaign in the study area. It was installed on the top of a water tank (~ 10 m) in the Lumbini International Research Institute (LIRI) premises, at a height that is unobstructed by buildings and trees. The sunphotometer made automatic measurements of direct-sun irradiance and sky radiance in eight spectral channels (340, 380, 440, 500, 675, 870, 940, and 1020 nm) to determine atmospheric transmission and scattering properties (Holben et al. 1998). AERONET data are available in three levels: level 1.0 (unscreened), level 1.5 (cloud screened), and level 2.0 (quality assured data) (Smirnov et al. 2009). Level 2.0 data collected between January 2013 and December 2014 (total 202 days; winter 23, pre-monsoon 80, monsoon 44, and post-monsoon 55 days) were used in the present study. The data used for this study were collected between January–August 2013 and September–December 2014. Despite the data gaps (mostly due to instrumental malfunction), we still believe this dataset is meaningful, especially considering the good quality data for most seriously polluted seasons like pre-monsoon and post-monsoon when agro-residue fires and forest fires, and agro-residue fires, respectively, are prevalent in the region.

Results and discussions

Overview of AOD and *α*

The AOD is a measure of aerosols from the surface of the earth to the top of the atmosphere and is defined as the extinction of solar radiation by atmospheric aerosols (Xin et al. 2014). The average AOD (at 500 nm) during the entire study period was found to be 0.64 ± 0.38 (0.06–3.28). In order to get insights on the AOD level, the values were compared with other AERONET sites over the IGP region and elsewhere as presented in Table 1. It is observed that the AOD levels over Lumbini are lower than in Delhi (0.82) (Sharma et al. 2014) but similar to Kanpur (0.62) (Kedia et al. 2014). Delhi is one

Table 1 Comparison of AOD and α over Lumbini with other sites in Asia. Values in italics refer to the fine-mode AOD

Location	Type	AOD	α	Sampling period	References
Lumbini	Semi-urban	0.58 ± 0.55 *0.53 ± 0.56*	1.34 ± 0.24 –	Winter	Present study
		0.66 ± 0.28 *0.47 ± 0.26*	1.14 ± 0.27 –	Pre-monsoon	
		0.31 ± 0.16 *0.31 ± 0.27*	1.19 ± 0.31 –	Monsoon	
		0.72 ± 0.44 *0.68 ± 0.43*	1.39 ± 0.12 –	Post-monsoon	
		0.64 ± 0.38 *0.54 ± 0.38*	1.24 ± 0.26 –	Entire study period	
Delhi	Urban	0.73 ± 0.10 0.67 ± 0.10	0.51 ± 0.16 1.02 ± 0.07	Summer Winter	(Srivastava et al. 2012a, b)
		0.82 ± 0.39	0.95 ± 0.37	2010–2012	(Sharma et al. 2014)
Lahore	Urban	0.54 ± 0.19 0.71 ± 0.46	– –	Pre-monsoon Post-monsoon	(Alam et al. 2014)
Kanpur Gandhi College	Urban Rural	0.62 ± 0.19 0.62 ± 0.16	0.98 ± 0.32 1.13 ± 0.27	2006–2010	(Kedia et al. 2014)
Kanpur Gandhi College	Urban Rural	0.50–0.69 0.51–0.77	0.45–0.74 0.65–0.91	Pre-monsoon	(Srivastava et al. 2011)
Varanasi	Semi-urban	0.2–1.8	0.25–1.8	2011	(Tiwari and Singh 2013)
Beijing	Urban	0.56–1.58	0.88–1.22	2005–2009	(Wang et al. 2011)
Taklimakan, China	Desert	< 0.3	0.55	Winter	(Che et al. 2013)
		0.75 0.65	~ 0.15 ~ 0.15	Spring Summer	
		< 0.3	0.36	Autumn	
Seoul, S. Korea Osaka, Japan	Urban Urban	0.43 0.30	1.20 1.27	DRAGON campaign Spring, 2012	(Kim et al. 2016)
EV-K2-CNR QOMS, Tibet	Remote Remote	0.04 0.05	– –	Annual Annual	(Xu et al. 2014)
Nam Co, Tibet	Remote	0.05	0.42 ± 0.27	Annual	(Cong et al. 2009)

of the megacities of Asia which lies near the Thar Desert and thus gets affected by the seasonal dust storms (Srivastava et al. 2014a). Similarly, the AOD in Lumbini is lower as compared to that from the largest sandy desert in the world, i.e., Taklimakan in China specifically during spring (0.75) and summer (0.65) seasons (Che et al. 2013). However, while comparing the aerosol loading at Lumbini with other megacities in East Asia, the AOD over Lumbini is observed to be higher than those over Seoul (0.43) and Osaka (0.30) (Kim et al. 2016) and more than ten times higher than that at the remote sites like Nam Co (inland Tibetan Plateau) and EvK2-CNR (Cong et al. 2009; Xu et al. 2014). Obviously, Lumbini as well as the surrounding regions possess very high aerosol loading, probably one of the highest in the world, implying serious effects on human health and climate system.

The Ångstrom exponent (α) is computed from a linear fit to the data pairs of the logarithm of AOD versus logarithm of the wavelength (Wang et al. 2011). A higher value of α indicates the dominance of fine particles mainly from the combustion-related anthropogenic sources, whereas lower values indicate the dominance of coarse particles like desert dust and sea salt (Alam et al. 2011b; Kaskaoutis et al. 2006; Lee et al. 2010; Srivastava et al. 2008; Wang et al. 2011). Therefore, α is a useful parameter to assess the size of atmospheric aerosols and thus to understand the wavelength dependence of the aerosol optical properties (Alam et al. 2011b; Lee et al. 2010; Srivastava et al. 2008; Wang et al. 2011). The average α over Lumbini during the whole study period was found to be 1.24 ± 0.26 (0.26–1.85). However, over Delhi (during summer), the α was found to be lower by more than half (0.51) of that observed in Lumbini indicating the presence of coarse particles transported from the nearby Thar Desert (Srivastava et al. 2012a). Over the North East Asia (during the DRAGON-NE campaign; spring of 2012), average α over Seoul was 1.20 and over Osaka it was 1.27 (Kim et al. 2016) which aids in understanding the influence of coarse-sized dust in and around the IGP region during spring or pre-monsoon season. Similarly, over a desert region, Che et al. (2013) reported even lower values of α. On the contrary, the higher values

of α over Lumbini as compared with other sites, like the background site at Nam Co, Tibet (Cong et al. 2009), indicate that the atmosphere over Lumbini is mostly affected by aerosols originated from anthropogenic activities or combustion sources (mainly biomass or fossil fuels).

Temporal variations of AOD and *α*, and comparison with the satellite data

The monthly average AOD, α, and columnar water vapor (CWV) during the measurement period (calculated from daily values) are shown in Fig. 2. Fog, haze, and cold waves are very common in the IGP region during winter (Kumar et al. 2015) and thus haze appears to have contributed to high values of AOD in the months of December (1.46 ± 0.78) and January (0.62 ± 0.10). As the pre-monsoon season advances, the aerosol loading starts increasing and the highest AOD value (during this season) is observed in June (0.93 ± 0.35). The lowest value of AOD during the study period was observed in July (0.25 ± 0.15). This phenomenon of sudden reduction in the AOD value during July is due to the washout of aerosols by heavy monsoon precipitation. A similar pattern of the AOD variation was observed in other IGP sites as well (Kedia et al. 2014; Sharma et al. 2014). It appears that the onset of the summer monsoon with southwesterly winds in South Asia pushes regional air pollution plumes in the IPG towards northern IGP, which increases AOD levels in early June. After the monsoon months, the aerosol loading in the atmosphere starts to increase. Regarding α, the highest average value was observed during the month of September (1.43 ± 0.15) during which the corresponding AOD was 0.46 ± 0.26. May was the month with lowest α (1.02 ± 0.23) with AOD value of 0.76 ± 0.25. Even though there exist some fluctuations in α values, but the values are high as compared to other AERONET sites in the IGP. The α during the pre-monsoon months over nearby IGP AERONET sites like Kanpur and Gandhi College were significantly lower (Kedia et al. 2014) than those in Lumbini, indicating the dominance of fine particles from anthropogenic activities in our site. Lumbini gets affected by both local and regional biomass burning over the IGP region during all seasons of the year but in considerable proportion during the non-monsoon seasons (Wan et al. 2017). These biomass burnings are also responsible for the occurrence of air pollution episodes during pre-monsoon in Lumbini (Rupakheti et al. 2017). Table 1 also shows the seasonal average fine-mode AOD over Lumbini, which explained why fine-mode AODs contribute to the total AOD to a large extent. High standard deviation seen in Fig. 2 and Table 1 refer to less data points (compared to other months) with fluctuating values due primarily to rain events. Finally, regarding CWV, it was lowest during the winter months, indicating dry winter in the study area; it started to increase during pre-monsoon and reached to the maximum value during the months of July (5.68 cm).

In order to compare the ground-based and satellite AOD, correlation between AOD obtained from these platforms has been studied. To maintain the consistency in data characteristics, AERONET AOD at 500 nm has been converted to AOD at 550 nm using spectral data as done in past studies (Alam et al. 2011a; Bibi et al. 2015). In this study, daily AOD data (over Lumbini) acquired with the MODIS instrument onboard the Aqua and Terra satellites have been retrieved from the Giovani data platform of NASA (http://giovanni.gsfc.nasa.gov/giovanni/). The same dataset was used earlier by Rupakheti et al. (2017) to study general air quality over Lumbini. Figure 3 shows the scatter plot representing daily AOD values as obtained by MODIS onboard both Terra and Aqua satellite and by the AERONET Cimel Sunphotometer for the year 2013–2014. The straight line fitting of AOD data from ground-based and Terra satellite resulted in an equation: $AOD_{Terra} = 0.88 \times AOD_{AERONET} + 0.08$ ($r = 0.79$), whereas that for

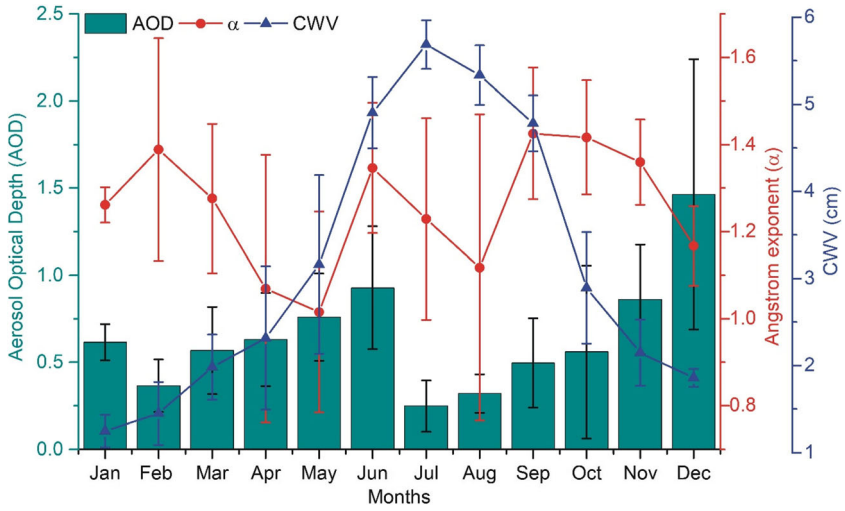

Fig. 2 Monthly average AOD, α, and CWV acquired with a CIMEL sunphotometer at Lumbini in northern Indo-Gangetic Plain in the period 2013–2014

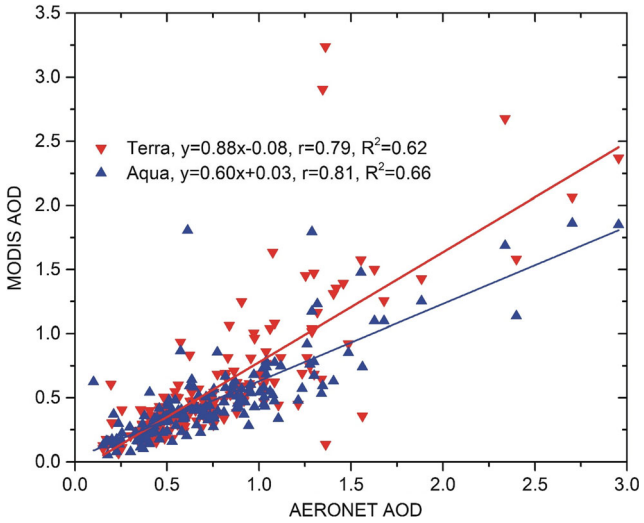

Fig. 3 Relationship between daily average AOD acquired with MODIS instrument onboard the satellite (Terra and Aqua) and AERONET Cimel Sunphotometer during the study period January 2013–December 2014

ground-based and Aqua satellite it was $AOD_{Aqua} = 0.60 \times AOD_{AERONET} + 0.03$ ($r = 0.81$). This indicates that the satellite instruments can detect majority of aerosol loading over the region. Similar correlation characteristics (low with Terra and high with Aqua) have also been reported for Gandhi College, a nearby AERONET site in IGP (Choudhry et al. 2012). The correlations obtained for Lumbini are lower than those observed over the Pearl River Delta (Xiao et al. 2017) and various sites under CARSNET in China (Xie et al. 2011) whereas higher than those observed over sites in central IGP (Choudhry et al. 2012) and Singapore (Chew et al. 2016) which needs investigation in future work.

The relationship between AOD and *α*

The scatter diagram of AOD vs α can be helpful in defining the physically interpretable cluster region for sources of different types of aerosols (Bi et al. 2011; Kaskaoutis et al. 2007; Smirnov et al. 2002). In Lumbini, both AOD and α values are spread over a wide range. In order to investigate the major aerosol types across the seasons, we have used the threshold that have been used earlier for another IGP site (Delhi, India) (Sharma et al. (2014); Tiwari et al. 2016). The threshold values of AOD and α for anthropogenic, mixed type, biomass burning, and dust were taken as 0.3–1.3 and >0.9, 0.4–0.7 and <0.9, >1.3 and >0.8, and >0.7 and <0.6 respectively. Aerosols with AOD and α values falling into groups other than the abovementioned categories were considered as undetermined aerosols.

Seasonal scatter diagrams of over 5410 instantaneous measurement values of AOD and α are presented in Fig. 4, which show various types of aerosols in Lumbini during different seasons. Dominant aerosol types can easily be understood from the figure like (i) clean conditions with AOD <0.2; (ii) higher values of AOD and α, representing biomass burning; and (iii) higher AOD but lower α that represents condition enriched with desert dust. Aerosols observed at Lumbini are

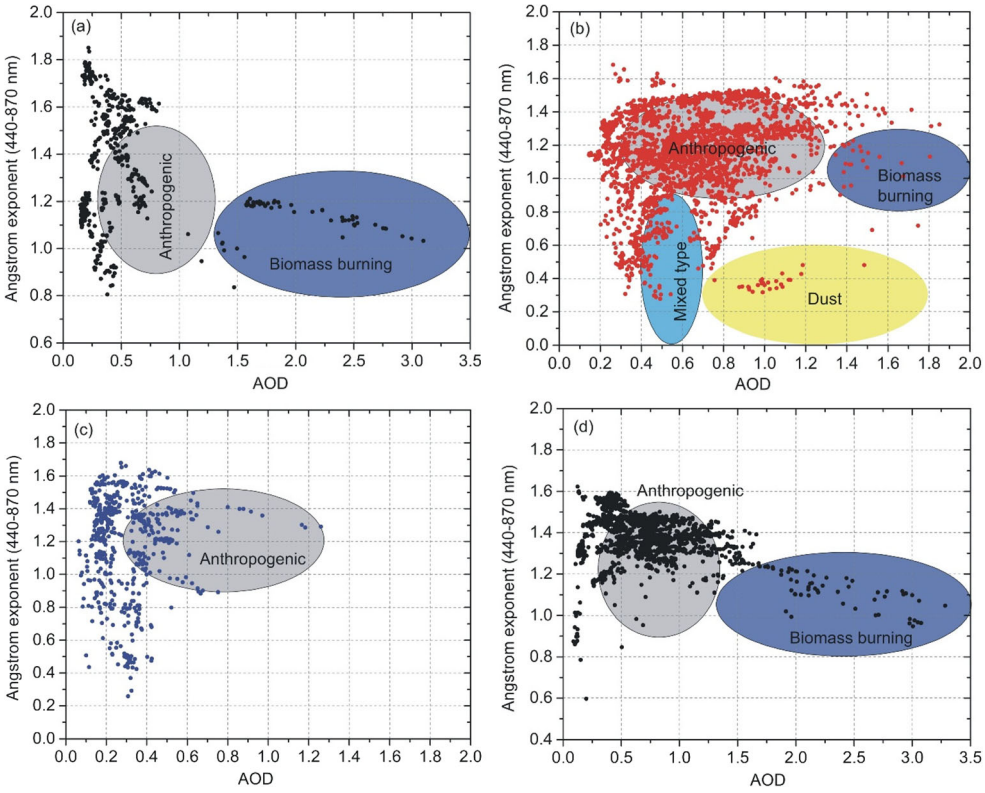

Fig. 4 Relationship between Angstrom exponent (α) and AOD observed during four seasons: **a** winter, **b** pre-monsoon, **c** monsoon, and **d** post-monsoon at Lumbini in the period 2013–2014

not predominantly from a single or same type of sources but are rather from multiple source type (marine, urban, desert, and biomass burning) as observed in another IGP site, Delhi (Sharma et al. 2014; Tiwari et al. 2016). Clean conditions with AOD < 0.2 were observed only during the monsoon season. Anthropogenic as well as undetermined aerosols were found in all four seasons with maximum number of data points during pre-monsoon. Very few data points only during the pre-monsoon season represented dust aerosols. Aerosols from biomass burning were found during the pre-monsoon and post-monsoon seasons as the IGP experiences frequent forest fires and agro-residue burning during these seasons (Habib et al. 2006; Kumar et al. 2016; Ramachandran and Cherian 2008; Rupakheti et al. 2017).

Season-based volume-size distribution of aerosols

The aerosol volume-size distribution (VSD), an important parameter to understand the radiative effect exerted by aerosols on the climate system (Alam et al. 2011b), was derived from the sun photometer measurements using 22 radius size bins ranging from 0.05 to 15 μm. The aerosol VSD has a bi-modal distribution which can be defined by the sum of two lognormal distributions, as governed by the following equation (Alam et al. 2012)

$$v(r) = \frac{dV(r)}{d\ln r} = \sum_{i=1}^{2} \frac{C_{v,i}}{\sqrt{2\pi}\sigma_i} \exp\left[\frac{-\left(\ln r - \ln r_{v,i}\right)}{2\sigma_i^2}\right]$$

where $C_{v,i}$ is the volume concentration for fine-mode and coarse-mode aerosols, σ_i is the geometric standard deviation for mode i, and $r_{v,i}$ is the volume mean radius.

Seasonal mean VSD for Lumbini are presented in Fig. 5, which show a clear bi-modal distribution of aerosols in each season. Mixing of air masses containing primary aerosols with fine and coarse-mode ones (Hoppel et al. 1985) or heterogeneous nucleation and growth of particle size through gas-to-particle conversion (Dey et al. 2005) lead to such bi-modal size distribution of aerosols. The fine-mode particles spread between 0.1 and 1 μm with peak centered between 0.1 and 0.3 μm, while the coarse-mode aerosols range from 1 to 10 μm with peak centered between 3 and 4 μm. VSD during the whole measurement period (not shown here) indicated that the volumetric concentration is higher in the fine-mode as compared to the coarse-mode ones implying the influence of anthropogenic sources in Lumbini. Among all seasons, post-monsoon had the highest volumetric concentration (~ 0.08 μm^{-3} μm^{-2} at its fine-mode peak) whereas the pre-monsoon had the highest volumetric concentration (~ 0.08 μm^{-3} μm^{-2} at its coarse-mode peak). The magnitudes of the fine-mode aerosols in each season are almost similar but different in the coarse-mode ones. Pre-monsoon and post-monsoon show the presence of coarse particles than in winter and monsoon. Moreover, the volumetric concentration in the coarse-mode fraction during pre-monsoon is more than double the concentrations during the winter and monsoon seasons. The highest volumetric concentration during pre-monsoon is due to the presence of coarse-mode dust particles, which are a common feature in IGP (Srivastava et al. 2011, 2014b). In addition, very little or no rainfall during this season in the region (Sigdel and Ma 2015) aids in the uplift of loose soil particles in the atmosphere resulting in high volumetric concentration in the coarse-mode particles. The changing wind pattern during different seasons (shown by the HYSPLIT diagrams as discussed later) also carried different types of aerosols generated over different regions to Lumbini which also influenced the aerosol VSD.

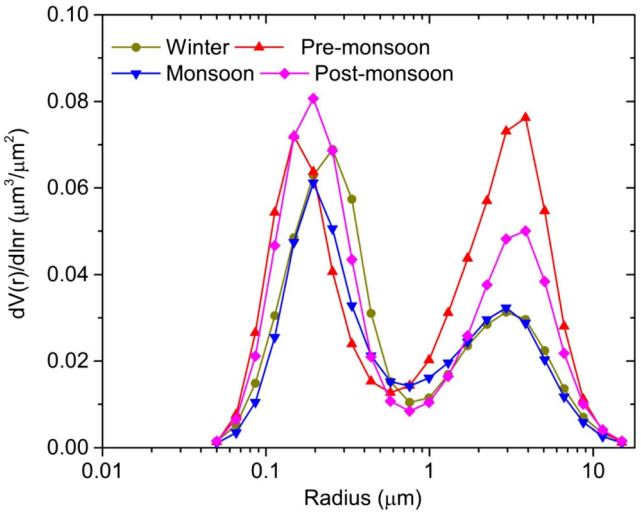

Fig. 5 Seasonal variation of aerosol volume-size distribution for different size bins ranging from 0.05 to 15 μm at Lumbini for all seasons in the period 2013–2014

The seasonal mean aerosol volume-size distribution parameters, including columnar volume concentration (V), effective radii (R_{eff}), volume mean radius (VMR), and geometric standard deviation (σ) for both fine-mode (f) and coarse-mode (c) particles is presented in Table 2. The volume concentration in fine modes (V_f) in all seasons are almost similar while V_c in pre-monsoon is nearly double the V_c during other seasons, suggesting the presence of coarse-mode aerosols during pre-monsoon, while the dominance of fine-mode aerosol is abundant in all seasons. Concerning the mean effective radius (R_{eff}) of the aerosol particles, no significant change across the seasons was observed in fine mode ($R_{eff,f}$) but significant change in the coarse-mode ($R_{eff,c}$). Such type of no significant/very minimal variation in effective radius (in fine mode) might have a greater optical effect (mostly in scattering efficiency) in comparison to the effective radii (in coarse mode), as observed over different sites in the IGP region (Tiwari et al. 2015). In addition to this, the difference in $R_{eff,c}$ across all seasons suggests large variability in the sources of coarse-mode aerosols (Srivastava et al. 2011).

Table 2 Summary of the VSD parameters of columnar aerosol loading over Lumbini. V is the volume concentration in μm^{-3} μm^{-3}, R_{eff} is the effective radius in micrometers, VMR is the volume median radius in micrometers, and σ is a geometric standard deviation for fine-mode (f) and coarse-mode (c) aerosols, respectively

Seasons	Parameters of VSD							
	V_f	$R_{eff,f}$	VMR_f	σ_f	V_c	$R_{eff,c}$	VMR_c	σ_c
Winter	0.09	0.18	0.20	0.50	0.05	2.28	2.79	0.65
Pre-monsoon	0.08	0.15	0.16	0.44	0.11	2.22	2.75	0.64
Monsoon	0.09	0.18	0.20	0.45	0.06	2.12	2.64	0.67
Post-monsoon	0.10	0.17	0.19	0.49	0.07	2.60	3.12	0.60

Aerosol radiative properties: single-scattering albedo, asymmetry parameter, and refractive index

Single-scattering albedo

The single-scattering albedo (SSA), a measure of light extinction due to scattering by aerosols, is an important parameter to understand the light scattering and absorbing properties of aerosols. It is determined from the ratio of the particle scattering coefficient to the total extinction coefficient (Bibi et al. 2016). SSA is strongly dependent upon the aerosol's chemical composition and size distribution (Dubovik et al. 2002). It is zero for pure absorption and one for pure scattering (Adesina et al. 2014; Kedia et al. 2014). Based on the worldwide AERONET stations, SSA values for different aerosol types have been reported as 0.78–0.94 for biomass burning aerosols, 0.83–0.98 for urban/industrial and mixed aerosols, and 0.92–0.99 for desert dust and marine aerosols (Dubovik et al. 2002). The seasonal average spectral variation of SSA at Lumbini is shown in Fig. 6 where the vertical bars represent one standard deviation. Seasonal average SSA values did not exhibit any significant spectral dependence. The highest SSA (~0.93 at 675 nm) was observed during the monsoon season, indicating the dominance of scattering aerosols. On the other hand, the lowest SSA (~0.82 at 675 nm) was observed in the post-monsoon season, indicating the presence of light-absorbing aerosols. Light-absorbing aerosols like elemental carbon (EC or often called BC) in total suspended particulate matter were found in highest concentration over Lumbini during post-monsoon as compared with that in other seasons (Wan et al. 2017). The SSA values suggest the presence of absorbing aerosols (except during monsoon), indicating highly absorbing atmosphere with SSA between 60 and 90%, as mentioned in Ramanathan and Ramana (2005), over Lumbini during other seasons. Gautam et al. (2011) also mentioned the presence of highly absorbing aerosols having SSA between 0.85 and 0.9 over the foothill/southern slope of Himalayas and remote sites in Nepal. Based on the SSA values observed in Lumbini, it can be inferred that the aerosols are highly absorbing in nature.

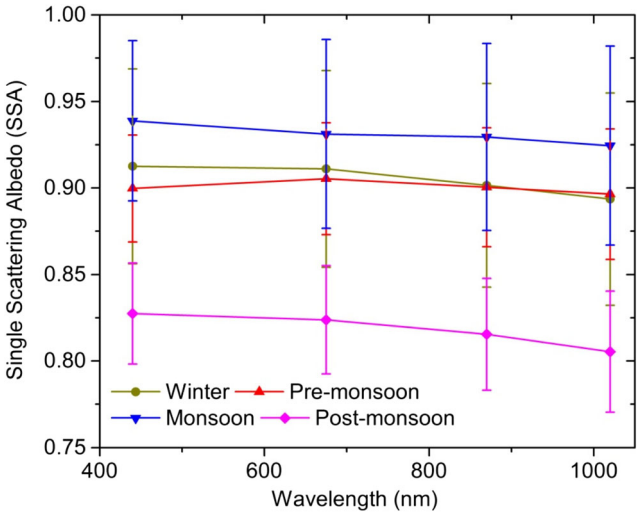

Fig. 6 Seasonal variation of SSA at four different wavelengths across four seasons at Lumbini in the period 2013–2014

In addition, the absorption AOD (AAOD) can be derived by using the formula mentioned in Bergstrom et al. (2007) and Russell et al. (2010).

$$AAOD_\lambda = (1-SSA_\lambda)\ AOD_\lambda$$

where λ is the wavelength. Over each season, the AAOD shows decreasing trend with increasing λ. Also, the absorption Ångstrom exponent (AAE) has been computed in the range of 440–1020 nm using the formula given by Mallet et al. (2013) as

$$AAE = \log\left(AAOD_{\lambda 1}/AAOD_{\lambda 2}\right)/\log\left(\lambda_2/\lambda_1\right)$$

Figure 7 shows the dependence of AAOD on wavelength, and the corresponding AAE values for each season. Russell et al. (2010) reported AAE values close to 1 for the US East Coast influenced by diesel exhausts during summer, 1.45 for biomass burning in South Africa, 2.27 and 2.34 for aerosols containing mineral dust later mixed with Asian dust and air pollution. In the case of Lumbini, the seasonal mean AAE values ranged between 0.92 (monsoon) and 1.27 (post-monsoon). Enhancement of AAE value over 1.0, a theoretical value of BC from diesel

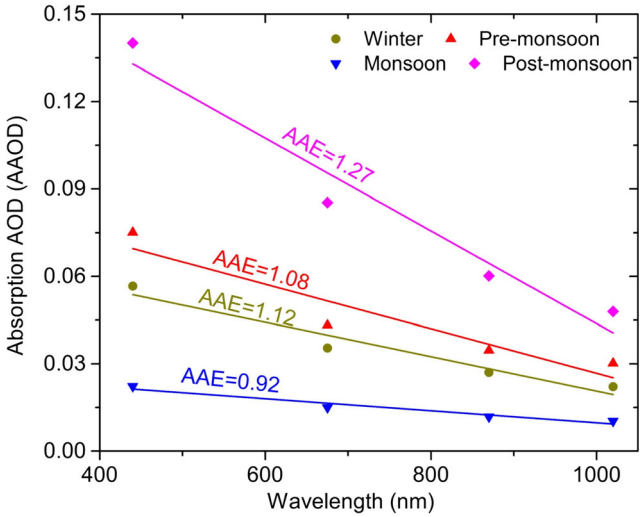

Fig. 7 Spectral variation of AAOD derived from AERONET's Cimel sunphotometer measurements at Lumbini across seasons in the period 2013–2014

combustion (Bergstrom et al. 2007), was observed in Lumbini in three seasons except monsoon, a finding similar to observations at other IGP sites in India (Srivastava et al. 2011). Praveen et al. (2012) have reported AAE values ranging between 1 and 2 for measurements at a village (Sultanpur) in Uttar Pradesh, about 170 km southwest of Lumbini, and referred to as presence of mixed aerosols from fossil fuel combustion and biomass burning. A recent study based on the source apportionment of BC observed with an Aethalometer during pre-monsoon in Lumbini by Rupakheti et al. (2017) has shown that the contribution of biomass burning and fossil fuel combustion emissions to total BC was, on average, 40 and 60%, respectively. Li et al. (2016) used carbon isotopes to quantify the BC source contribution and found that the fossil fuel combustion contributed for about 50% of BC in Lumbini. Based on this, we can confirm the source of aerosol in Lumbini as originated from both biomass burning and fossil fuel combustion.

Asymmetry parameter (g) and refractive index

The asymmetry parameter (AP) (g) is the angular distribution of light scattered by aerosol particles calculated as follows (Andrews et al. 2006).

$$g = \frac{1}{2}\int_0^{\pi} \cos\theta P(\theta) \sin\theta \, d\theta$$

where θ is the angle between incident light and scattering direction and $P(\theta)$ is the angular distribution of scattered light or the phase function. The value of g ranges from − 1 (radiation is entirely backscattered) to + 1 (entirely forward scattered radiation) and is dependent, just like SSA, upon the size and composition of the particles in the atmosphere (Andrews et al. 2006; Tiwari et al. 2015). The seasonal variation of g measured at different wavelengths is shown in Fig. 8. A uniform decrease in g values with increasing wavelengths is observed indicating its spectral dependence. During winter, monsoon, and post-monsoon seasons, the g value decreases monotonically over both visible and infrared (IR) spectral regions but in the pre-monsoon season, it slightly increases over the IR region. Tiwari et al. (2015) reported that for dust or polluted continental aerosols the asymmetry parameter exhibits such behavior. Namely, the increase of the g values over the IR range indicates the presence of coarse particles (Bibi et al. 2016). This means that the pre-monsoon aerosols observed at Lumbini are a mix of dust (in coarse mode) and continental air pollution. Moreover, the overall decrease in the asymmetry parameter during winter, monsoon, and post-monsoon seasons indicates the presence of fine particles in the atmosphere. The average g value ranges from 0.71 to 0.75 at 440 nm whereas between 0.59 and 0.62 at 1020 nm. A similar pattern of spectral change and extent of g values in the 1020 nm channel has been identified as either BC enriched or OC enriched aerosols in the IGP (Tiwari et al. 2015). The highest g values at both of the aforementioned channels (440 and 1020 nm) were observed during the monsoon season and the lowest values during the pre-monsoon (post-monsoon at highest wavelength), suggesting the presence of anthropogenic or absorbing aerosols in abundance.

The real and imaginary parts of the aerosol refractive index (RI) also depend upon their chemical composition (Bibi et al. 2016). They are useful in understanding the scattering and absorption of the incoming solar radiation (Adesina et al. 2014; Singh et al. 2004) with higher values of the real and imaginary parts indicating light scattering

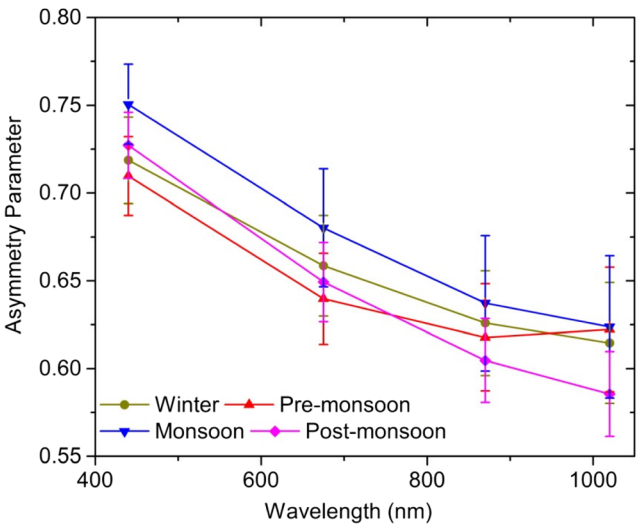

Fig. 8 Spectral variation of g at four wavelengths derived from AERONET's Cimel sunphotometer at Lumbini for all seasons in the period 2013–2014

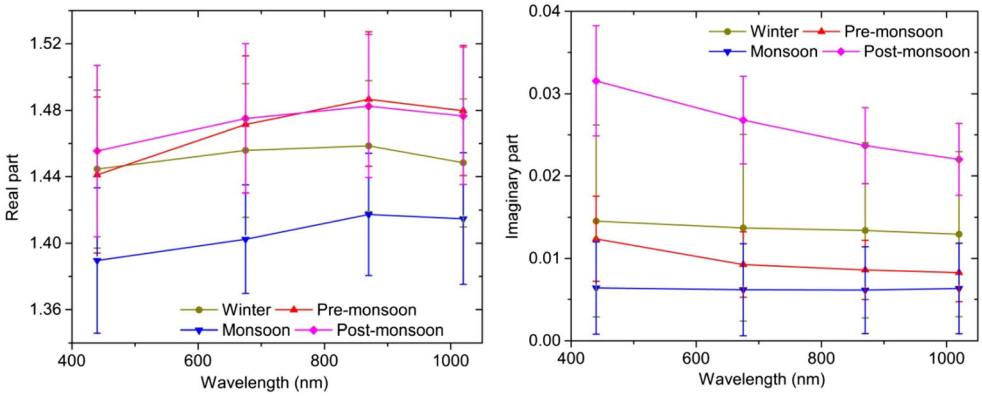

Fig. 9 Spectral variation of aerosol RI [real part (left panel) and imaginary part (right panel)] at 440, 675, 870, and 1020 nm across different seasons in Lumbini in the period 2013–2014

and light-absorbing aerosols, respectively (Alam et al. 2012; Bibi et al. 2016; Singh et al. 2004; Sinyuk et al. 2003). Dubovik et al. (2002) have reported the values of the real part of RI to range in 1.40–1.47 for urban-industrial and mixed aerosols, in 1.47–1.52 for biomass burning, and in 1.36–1.56 for desert dust, whereas the values of the imaginary part of RI to range in 0.003–0.014, 0.00093–0.021, and 0.0007–0.0029, respectively, for these three different sources. Figure 9 shows the seasonal averages of the real and imaginary parts of RI observed at Lumbini. The real part increases from 440 to 870 nm, with a peak value at 870 nm, and again lower value at 1020 nm during all seasons. This spectral pattern is similar to other sites in the IGP region (Bibi et al. 2016). Higher values of the real part of RI during pre-monsoon and post-monsoon seasons could be attributed to the higher concentrations of carbonaceous aerosols present during these seasons in Lumbini (Wan et al. 2017). Average values of the real part are 1.44, 1.44, 1.39, and 1.46 at 440 nm and 1.45, 1.48, 1.41, and 1.44 at 1020 nm during winter, pre-monsoon, monsoon, and post-monsoon seasons, respectively. The highest value of the real part at larger wavelengths (> 670 nm), as shown in the figure, indicates higher scattering (Bibi et al. 2016; Singh et al. 2004). In addition, the lowest values of the real part during the monsoon season might have been associated with high relative humidity and thus hygroscopic growth of the aerosol.

Moreover, the values of the imaginary part were found to be 0.0145, 0.0124, 0.0064, and 0.0316 at 440 nm and 0.0129, 0.0083, 0.0063, and 0.0220 at 1020 nm, respectively, for all seasons. Regarding the imaginary part of the RI, its values are higher as compared to those observed over other IGP sites (Bibi et al. 2016), indicating the presence of more light-absorbing aerosols over Lumbini. The imaginary part did not change with wavelengths during winter and monsoon, whereas during pre-monsoon and post-monsoon, its values reduced with increasing wavelength, in a more rapid rate during post-monsoon. This nature of imaginary part of RI (during pre-monsoon and post-monsoon season) could be attributed to the absorption of fine particulates (both OC and BC) (Arola et al. 2011).

Air masses arriving at the study site: HYSPLIT back trajectory

Back trajectory analysis has been carried out in order to understand the possible origin regions and transport pathways of air masses and air pollution (Kang et al. 2016; Kaskaoutis et al. 2012; Kaskaoutis et al. 2010; Srivastava et al. 2012b; Tripathee et al. 2016). Five-day air-mass back-trajectories were plotted using the Hybrid Single-Particle Lagrangian Integrated Trajectory (HYSPLIT) model from the Air Resources Laboratory of National Oceanic and Atmospheric Administration (NOAA, http://www.arl.noaa.gov/HYSPLIT_info.php). Seasonal mean trajectories were calculated for air masses arriving at the site at the height of 500 m or within the mixed layer height in the region. Figure 10 shows the mean trajectories, ending at Lumbini for the studied seasons. During the winter and pre-monsoon, westerly winds are prevalent (about 90 and 60% of the air masses in the respective seasons). About 75% of the air masses that reached Lumbini were from the northwestern IGP region and ~ 15% of the air masses originated in mid-east Asia (Iraq) during winter. In the pre-monsoon season, air masses passing over the eastern part of Nepal and northern India near the India-Nepal boarder (41%), some from the local regions, i.e., from the Nepalese part of IGP and Indian part of IGP to the west of Lumbini (28%), and a considerable fraction (29%) from Pakistan were observed. Biomass for cooking activities and crop residue burning is common in IGP region (Ganguly et al. 2006; Gautam et al. 2011; Sharma et al. 2010; Singh et al. 2014; Srivastava et al. 2012b). Thus, the air masses originated in or traveling through north Indian states like Punjab and Haryana carry aerosols generated from such biomass burning activities. Figure 10 also shows the active open fires over south Asian region in different seasons during the study period. Regarding the fires over IGP, the northwest IGP region is found to be having a higher number of such fires. Likewise, the highest number of fires occurred during the pre-monsoon season in northeastern Pakistan, northwestern India, and in the foothills of the Himalayas in India and Nepal is responsible for the higher loading of aerosols during this season. It has been also

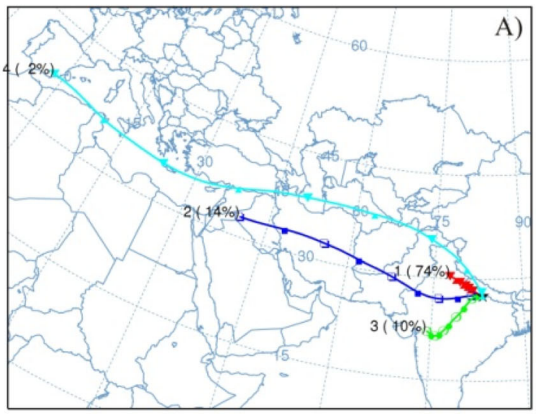
A)
4 (2%)
2 (14%)
1 (74%)
3 (10%)

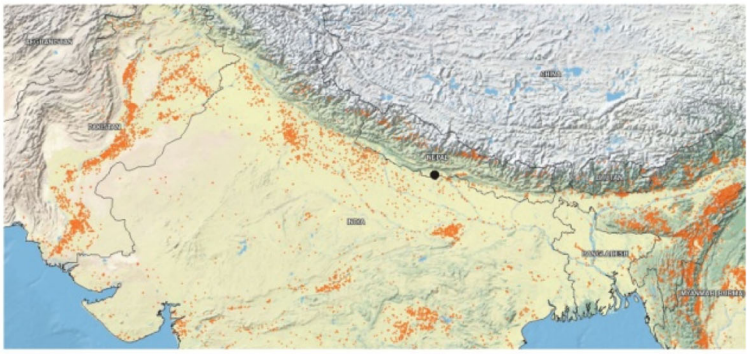

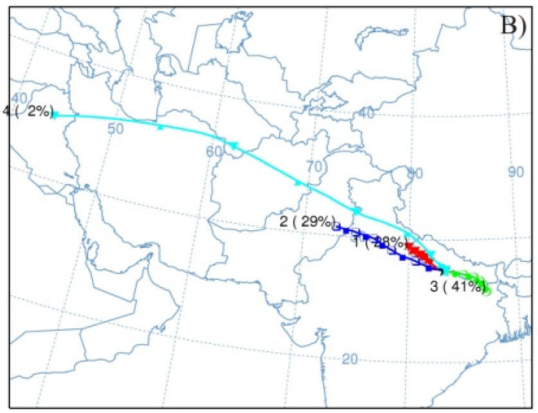
B)
4 (2%)
2 (29%)
3 (41%)

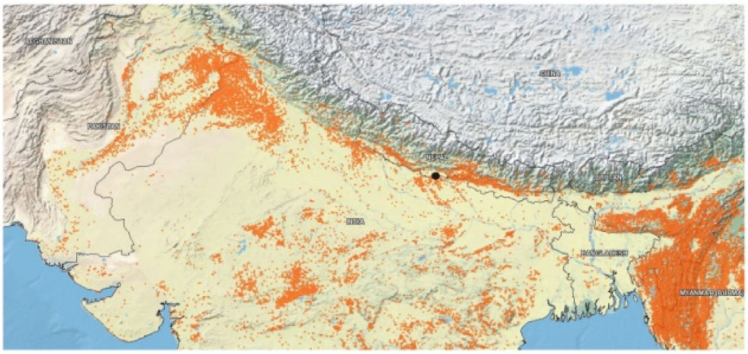

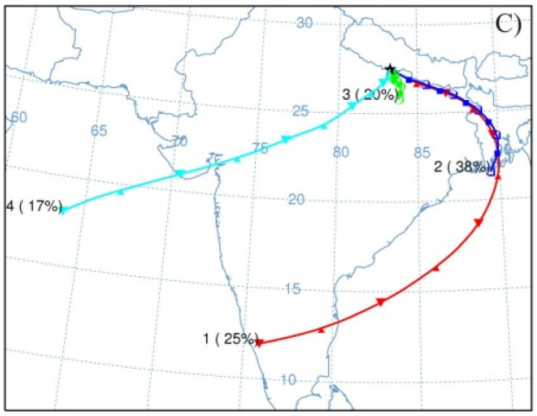
C)
3 (20%)
2 (38%)
4 (17%)
1 (25%)

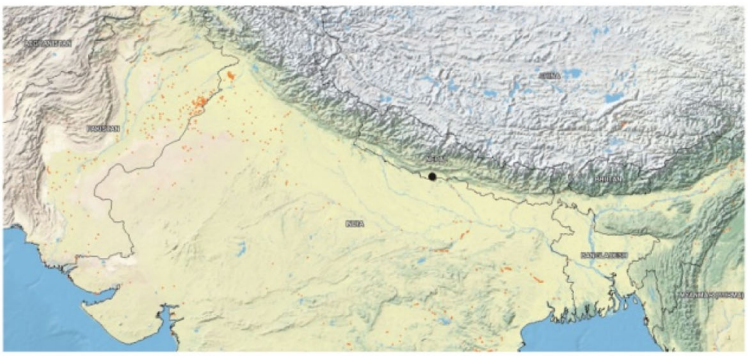

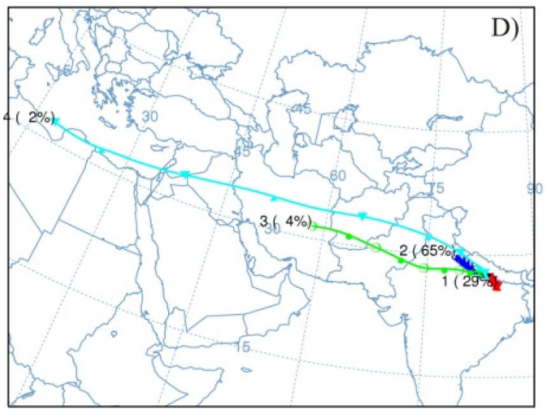
D)
4 (2%)
3 (4%)
2 (65%)
1 (29%)

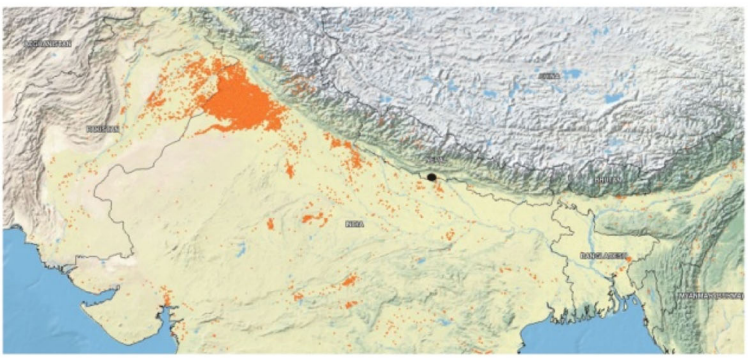

reported in a previous study that fires in the north Indian plains are responsible for the higher loading of aerosols even over the northern slope of the Himalayas (Cong et al. 2015). But during monsoon, the air masses were mostly from east and southeast directions including air masses passing over Bangladesh, which traveled afterwards through the eastern IGP in India before reaching Lumbini in Nepal. These air masses might have transported the aerosols emitted over the eastern IGP region before arriving in the study area. During the post-monsoon season, about 70% of the air masses was either originated or traveled through the northwestern IGP region, which carried the biomass or crop residue burning emissions over these regions to the study site. Post-harvest crop residue burning (mainly rice straw) occurs during post-monsoon mainly over the northwestern IGP region, which emits huge amounts of gaseous and particulate air pollutants (Kumar et al. 2016; Sarkar et al. 2013; Sinha et al. 2014).

Conclusions

For the first time, the AERONET's CIMEL sunphotometer was deployed in Lumbini, southern lowland Nepal—a site at the northern edge of the Indo-Gangetic Plain (IGP) for a period of nearly 2 years during January 2013–December 2014. Key aerosol optical properties (AOD, α, VSD, SSA, g) were studied from the available dataset. The instantaneous value of AOD was found to be in the range of 0.06–3.28 with an average of 0.64 ± 0.38 over the entire sampling period of 202 days (over almost 2-year period) that encompasses part of both dry and rainy season in south Asia. The highest aerosol loading (seasonal average) was observed during post-monsoon with an average AOD value of 0.72 ± 0.44 (0.09–3.28). As inferred from α values, anthropogenic (fine) aerosols were found to be higher over Lumbini as compared to other nearby IGP sites. More than 80% of the daily averaged AOD values were above 0.3, indicating that Lumbini and the surrounding region are polluted. Lumbini also experiences anthropogenic aerosols and from biomass burning activities in three seasons (winter, monsoon, and post-monsoon). In addition to these aerosols, wind-blown dust was also observed during pre-monsoon. Most of the air masses reaching the Lumbini site either originated or traveled through heavily aerosol-laden areas in IGP region (mostly northwestern IGP) during the study period. Anthropogenic, mixed, and undetermined and those of biomass burning origin constituted the major aerosol types in Lumbini. The SSA analysis suggested that the columnar aerosol loading in Lumbini is dominated by absorbing aerosols. In addition, analysis of g and RI also confirmed that the aerosols over Lumbini were mostly of anthropogenic origin (from urban/industrial and biomass burning). The aerosol VSDs showed a bi-modal distribution with varying total and modal volume concentrations (highest during post-monsoon in fine-mode and during pre-monsoon in coarse-mode). As this is the first study of this kind in lowland Nepal, it provides unique insights on the optical properties of aerosols in the pollution outflows from the heavily polluted Indo-Gangetic Plain that gets advected towards the foothills of the Himalayas and remote mountainous regions in the Himalayan-Tibetan region. We suggest that long-term monitoring of the aerosol optical properties at this site as well as others along a couple of north-south transects from IGP to the Tibetan Plateau is essential for advancing our knowledge on the type, accumulation in the southern flank of the Himalayas, transport (horizontal and vertical), transformation, and removal of aerosols, and their impacts on the Himalaya and Tibetan Plateau regions with sensitive ecosystems of regional and global significance.

◀ **Fig. 10** Five-day average air-mass back-trajectories computed with HYSPLIT model for **a** winter, **b** pre-monsoon, and **c** monsoon of 2013, and **d** post-monsoon season of 2014 at the altitude of 500 m above ground at Lumbini (27.49° N and 83.28° E). The images of the right panels show the distribution of open fires (images acquired from MODIS https://firms.modaps.eosdis.nasa.gov/firemap/). The black dots in the right panels indicate the location of Lumbini

Acknowledgements Maheswar Rupakheti acknowledges the support provided by the Institute for Advanced Sustainability Studies (IASS) which is funded by the German Federal Ministry for Education and Research (BMBF) and the Brandenburg Ministry for Science, Research and Culture (MWFK). The authors acknowledge Christoph Cüppers and Michael Pahlke of the Lumbini International Research Institute (LIRI) for providing the space and power to run the instruments at the LIRI premises and Bhogendra Kathayat and Bhoj Raj Bhatta for their support in the operation of the site.

Funding information This study is supported by National Natural Science Foundation of China (41630754 and 41721091), Chinese Academy of Sciences (QYZDJ-SSW-DQC039) and the State Key Laboratory of Cryospheric Science (SKLCS-ZZ-2017). Dipesh Rupakheti is supported by CAS-TWAS President's Fellowship for International PhD Students.

References

Adesina AJ, Kumar KR, Sivakumar V, Griffith D (2014) Direct radiative forcing of urban aerosols over Pretoria (25.75° S, 28.28° E) using AERONET sunphotometer data: first scientific results and environmental impact. J Environ Sci 26:2459–2474

Adhikary B, Carmichael GR, Tang Y, Leung LR, Qian Y, Schauer JJ, Stone EA, Ramanathan V, Ramana MV (2007) Characterization of the seasonal cycle of south Asian aerosols: a regional-scale modeling analysis. J Geophys Res 112(D22S22):1–22

Alam K, Qureshi S, Blaschke T (2011a) Monitoring spatio-temporal aerosol patterns over Pakistan based on MODIS, TOMS and MISR satellite data and a HYSPLIT model. Atmos Environ 45: 4641–4651

Alam K, Trautmann T, Blaschke T (2011b) Aerosol optical properties and radiative forcing over mega-city Karachi. Atmos Res 101:773–782

Alam K, Trautmann T, Blaschke T, Majid H (2012) Aerosol optical and radiative properties during summer and winter seasons over Lahore and Karachi. Atmos Environ 50:234–245

Alam K, Khan R, Ali S, Ajmal M, Khan G, Muhammad W, Ali MA (2014) Variability of aerosol optical depth over Swat in Northern Pakistan based on satellite data. Arab J Geosci 8:547–555

Andrews E, Sheridan P, Fiebig M, McComiskey A, Ogren J, Arnott P, Covert D, Elleman R, Gasparini R, Collins D (2006) Comparison of methods for deriving aerosol asymmetry parameter. J Geophys Res 111:1–16

Arola A, Schuster G, Myhre G, Kazadzis S, Dey S, Tripathi SN (2011) Inferring absorbing organic carbon content from AERONET data. Atmos Chem Phys 11:215–225

Bergstrom RW, Pilewskie P, Russell P, Redemann J, Bond T, Quinn P, Sierau B (2007) Spectral absorption properties of atmospheric aerosols. Atmos Chem Phys 7:5937–5943

Bi J, Huang J, Fu Q, Wang X, Shi J, Zhang W, Huang Z, Zhang B (2011) Toward characterization of the aerosol optical properties over Loess Plateau of Northwestern China. J Quant Spectrosc Radiat Transf 112:346–360

Bibi H, Alam K, Chishtie F, Bibi S, Shahid I, Blaschke T (2015) Intercomparison of MODIS, MISR, OMI, and CALIPSO aerosol optical depth retrievals for four locations on the Indo-Gangetic plains and validation against AERONET data. Atmos Environ 111:113–126

Bibi H, Alam K, Blaschke T, Bibi S, Iqbal MJ (2016) Long-term (2007–2013) analysis of aerosol optical properties over four locations in the Indo-Gangetic plains. Appl Opt 55:6199–6211

Che H, Wang Y, Sun J, Zhang X, Zhang X, Guo J (2013) Variation of aerosol optical properties over the Taklimakan Desert in China. Aerosol Air Qual Res 13:777–785

Chew BN, Campbell JR, Hyer EJ, Salinas SV, Reid JS, Welton EJ, Holben BN, Liew SC (2016) Relationship between aerosol optical depth and particulate matter over Singapore: effects of aerosol vertical distributions. Aerosol Air Qual Res 16:2818–2830

Choudhry P, Misra A, Tripathi S (2012) Study of MODIS derived AOD at three different locations in the Indo Gangetic Plain: Kanpur, Gandhi College and Nainital, Annales Geophysicae. Copernicus GmbH, pp. 1479–1493

Cong Z, Kang S, Smirnov A, Holben B (2009) Aerosol optical properties at Nam Co, a remote site in central Tibetan Plateau. Atmos Res 92:42–48

Cong Z, Kang S, Kawamura K, Liu B, Wan X, Wang Z, Gao S, Fu P (2015) Carbonaceous aerosols on the south edge of the Tibetan Plateau: concentrations, seasonality and sources. Atmos Chem Phys 15:1573–1584

Dey S, Tripathi SN, Singh RP, Holben BN (2005) Seasonal variability of the aerosol parameters over Kanpur, an urban site in Indo-Gangetic basin. Adv Space Res 36:778–782

Dubovik O, Holben B, Eck TF, Smirnov A, Kaufman YJ, King MD, Tanré D, Slutsker I (2002) Variability of absorption and optical properties of key aerosol types observed in worldwide locations. J Atmos Sci 59:590–608

Ganguly D, Jayaraman A, Rajesh TA, Gadhavi H (2006) Wintertime aerosol properties during foggy and nonfoggy days over urban center Delhi and their implications for shortwave radiative forcing. J Geophys Res 111:1–15

Gautam R, Hsu NC, Lau KM, Tsay SC, Kafatos M (2009) Enhanced pre-monsoon warming over the Himalayan-Gangetic region from 1979 to 2007. Geophys Res Lett 36:1–5

Gautam R, Hsu NC, Tsay SC, Lau KM, Holben B, Bell S, Smirnov A, Li C, Hansell R, Ji Q, Payra S, Aryal D, Kayastha R, Kim KM (2011) Accumulation of aerosols over the Indo-Gangetic plains and southern slopes of the Himalayas: distribution, properties and radiative effects during the 2009 pre-monsoon season. Atmos Chem Phys 11:12841–12863

Gobbi GP, Angelini F, Bonasoni P, Verza GP, Marinoni A, Barnaba F (2010) Sunphotometry of the 2006–2007 aerosol optical/radiative properties at the Himalayan Nepal climate observatory-pyramid (5079 m a.s.l.) Atmos Chem Phys 10:11209–11221

Habib G, Venkataraman C, Chiapello I, Ramachandran S, Boucher O, Shekar Reddy M (2006) Seasonal and interannual variability in absorbing aerosols over India derived from TOMS: relationship to regional meteorology and emissions. Atmos Environ 40:1909–1921

Holben BN, Eck TF, Slutsker I, Tanré D, Buis JP, Setzer A, Vermote E, Reagan JA, Kaufman YJ, Nakajima T, Lavenu F, Jankowiak I, Smirnov A (1998) AERONET—a federated instrument network and data archive for aerosol characterization. Remote Sens Environ 66:1–16

Hoppel WA, Fitzgerald JW, Larson RE (1985) Aerosol size distributions in air masses advecting off the east coast of the United States. J Geophys Res 90:2365–2379

Kang S, Chen P, Li C, Liu B, Cong Z (2016) Atmospheric aerosol elements over the inland Tibetan Plateau: concentration, seasonality, and transport. Aerosol Air Qual Res 16:789–800

Kaskaoutis D, Kambezidis H, Adamopoulos A, Kassomenos P (2006) On the characterization of aerosols using the Ångström exponent in the Athens area. J Atmos Sol Terr Phys 68:2147–2163

Kaskaoutis D, Kambezidis H, Hatzianastassiou N, Kosmopoulos P, Badarinath K (2007) Aerosol climatology: on the discrimination of aerosol types over four AERONET sites. Atmos Chem Phys Discuss 7:6357–6411

Kaskaoutis DG, Nastos PT, Kosmopoulos PG, Kambezidis HD (2010) The combined use of satellite data, air-mass trajectories and model applications for monitoring dust transport over Athens, Greece. Int J Remote Sens 31:5089–5109

Kaskaoutis D, Kosmopoulos P, Nastos P, Kambezidis H, Sharma M, Mehdi W (2012) Transport pathways of Sahara dust over Athens, Greece as detected by MODIS and TOMS. Geomat Nat Haz Risk 3:35–54

Kaufman YJ, Tanré D, Boucher O (2002) A satellite view of aerosols in the climate system. Nature 419:215–223

Kedia S, Ramachandran S, Holben BN, Tripathi SN (2014) Quantification of aerosol type, and sources of aerosols over the Indo-Gangetic Plain. Atmos Environ 98:607–619

Kim M, Kim J, Jeong U, Kim W, Hong H, Holben B, Eck TF, Lim JH, Song CK, Lee S, Chung CY (2016) Aerosol optical properties derived from the DRAGON-NE Asia campaign, and implications for a single-channel algorithm to retrieve aerosol optical depth in spring from meteorological imager (MI) on-board the communication, ocean, and meteorological satellite (COMS). Atmos Chem Phys 16:1789–1808

Kumar M, Tiwari S, Murari V, Singh AK, Banerjee T (2015) Wintertime characteristics of aerosols at middle Indo-Gangetic Plain: impacts of regional meteorology and long range transport. Atmos Environ 104:162–175

Kumar V, Sarkar C, Sinha V (2016) Influence of post-harvest crop residue fires on surface ozone mixing ratios in the NW IGP analyzed using 2 years of continuous in situ trace gas measurements. J Geophys Res 121:3619–3633

Lee J, Kim J, Song CH, Kim SB, Chun Y, Sohn BJ, Holben BN (2010) Characteristics of aerosol types from AERONET sunphotometer measurements. Atmos Environ 44:3110–3117

Li C, Bosch C, Kang S, Andersson A, Chen P, Zhang Q, Cong Z, Chen B, Qin D, Gustafsson Ö (2016) Sources of black carbon to the Himalayan–Tibetan Plateau glaciers. Nat Commun 7:12574

Lüthi ZL, Škerlak B, Kim SW, Lauer A, Mues A, Rupakheti M, Kang S (2015) Atmospheric brown clouds reach the Tibetan Plateau by crossing the Himalayas. Atmos Chem Phys 15:6007–6021

Mallet M, Dubovik O, Nabat P, Dulac F, Kahn R, Sciare J, Paronis D, Léon JF (2013) Absorption properties of Mediterranean aerosols obtained from multi-year ground-based remote sensing observations. Atmos Chem Phys 13:9195–9210

Marcq S, Laj P, Roger J, Villani P, Sellegri K, Bonasoni P, Marinoni A, Cristofanelli P, Verza G, Bergin M (2010) Aerosol optical properties and radiative forcing in the high Himalaya based on measurements at the Nepal Climate Observatory-Pyramid site (5079 m asl). Atmos Chem Phys 10:5859–5872

Mehta M (2015) A study of aerosol optical depth variations over the Indian region using thirteen years (2001–2013) of MODIS and MISR level 3 data. Atmos Environ 109:161–170

Praveen PS, Ahmed T, Kar A, Rehman IH, Ramanathan V (2012) Link between local scale BC emissions in the Indo-Gangetic Plains and large scale atmospheric solar absorption. Atmos Chem Phys 12: 1173–1187

Ram K, Sarin MM (2011) Day–night variability of EC, OC, WSOC and inorganic ions in urban environment of Indo-Gangetic Plain: implications to secondary aerosol formation. Atmos Environ 45:460–468

Ram K, Sarin MM (2015) Atmospheric carbonaceous aerosols from Indo-Gangetic Plain and central Himalaya: impact of anthropogenic sources. J Environ Manag 148:153–163

Ramachandran S, Cherian R (2008) Regional and seasonal variations in aerosol optical characteristics and their frequency distributions over India during 2001–2005. J Geophys Res 113:1–16

Ramanathan V, Carmichael G (2008) Global and regional climate changes due to black carbon. Nat Geosci 1:221–227

Ramanathan V, Crutzen PJ (2003) New directions: atmospheric Brown "clouds". Atmos Environ 37:4033–4035

Ramanathan V, Ramana MV (2005) Persistent, widespread, and strongly absorbing haze over the Himalayan foothills and the Indo-Gangetic Plains. Pure Appl Geophys 162:1609–1626

Ramanathan V, Crutzen PJ, Kiehl JT, Rosenfeld D (2001) Aerosols, climate, and the hydrological cycle. Science 294:2119–2124

Rosenfeld D (2000) Suppression of rain and snow by urban and industrial air pollution. Science 287:1793–1796

Rupakheti D, Adhikary B, Praveen PS, Rupakheti M, Kang S, Mahata KS, Naja M, Zhang Q, Panday AK, Lawrence MG (2017) Premonsoon air quality over Lumbini, a world heritage site along the Himalayan foothills. Atmos Chem Phys 17:11041–11063

Russell P, Bergstrom R, Shinozuka Y, Clarke A, DeCarlo P, Jimenez J, Livingston J, Redemann J, Dubovik O, Strawa A (2010) Absorption Angstrom xponent in AERONET and related data as an indicator of aerosol composition. Atmos Chem Phys 10:1155–1169

Sarkar C, Kumar V, Sinha V (2013) Massive emissions of carcinogenic benzenoids from paddy residue burning in north India. Curr Sci India 104:1703–1709

Sharma AR, Kharol SK, Badarinath K, Singh D (2010) Impact of agriculture crop residue burning on atmospheric aerosol loading—a study over Punjab State, India. Ann Geophys 28:367–379

Sharma M, Kaskaoutis DG, Singh RP, Singh S (2014) Seasonal variability of atmospheric aerosol parameters over Greater Noida using ground sunphotometer observations. Aerosol Air Qual Res 14:608–622

Shrestha P, Barros AP, Khlystov A (2010) Chemical composition and aerosol size distribution of the middle mountain range in the Nepal Himalayas during the 2009 pre-monsoon season. Atmos Chem Phys 10:11605–11621

Sigdel M, Ma Y (2015) Evaluation of future precipitation scenario using statistical downscaling model over humid, subhumid, and arid region of Nepal—a case study. Theor Appl Climatol 123:1–8

Singh R, Dey S, Tripathi S, Tare V, Holben B (2004) Variability of aerosol parameters over Kanpur, northern India. J Geophys Res 109:1–14

Singh A, Rajput P, Sharma D, Sarin MM, Singh D (2014) Black carbon and elemental carbon from postharvest agricultural-waste burning emissions in the indo-Gangetic plain. Adv Meteorol 2014:1–10

Sinha V, Kumar V, Sarkar C (2014) Chemical composition of premonsoon air in the Indo-Gangetic Plain measured using a new air quality facility and PTR-MS: high surface ozone and strong influence of biomass burning. Atmos Chem Phys 14:5921–5941

Sinyuk A, Torres O, Dubovik O (2003) Combined use of satellite and surface observations to infer the imaginary part of refractive index of Saharan dust. Geophys Res Lett 30(2):1–4

Smirnov A, Holben BN, Dubovik O, O'Neill NT, Eck TF, Westphal DL, Goroch AK, Pietras C, Slutsker I (2002) Atmospheric aerosol optical properties in the Persian Gulf. J Atmos Sci 59:620–634

Smirnov A, Holben B, Slutsker I, Giles D, McClain CR, Eck T, Sakerin S, Macke A, Croot P, Zibordi G (2009) Maritime aerosol network as a component of aerosol robotic network. J Geophys Res Atmos 114

Srivastava A, Devara P, Rao YJ, Bhavanikumar Y, Rao D (2008) Aerosol optical depth, ozone and water vapor measurements over Gadanki, a tropical station in peninsular India. Aerosol Air Qual Res 8:459–476

Srivastava AK, Tiwari S, Devara PCS, Bisht DS, Srivastava MK, Tripathi SN, Goloub P, Holben BN (2011) Pre-monsoon aerosol characteristics over the Indo-Gangetic Basin: implications to climatic impact. Ann Geophys 29:789–804

Srivastava AK, Singh S, Tiwari S, Kanawade VP, Bisht DS (2012a) Variation between near-surface and columnar aerosol characteristics during the winter and summer at Delhi in the Indo-Gangetic Basin. J Atmos Sol-Terr Phys 77:57–66

Srivastava AK, Tripathi SN, Dey S, Kanawade VP, Tiwari S (2012b) Inferring aerosol types over the Indo-Gangetic Basin from ground based sunphotometer measurements. Atmos Res 109-110:64–75

Srivastava AK, Bisht DS, Ram K, Tiwari S, Srivastava MK (2014a) Characterization of carbonaceous aerosols over Delhi in Ganga basin: seasonal variability and possible sources. Environ Sci Pollut Res 21:8610–8619

Srivastava AK, Yadav V, Pathak V, Singh S, Tiwari S, Bisht DS, Goloub P (2014b) Variability in radiative properties of major aerosol types: a year-long study over Delhi—an urban station in Indo-Gangetic Basin. Sci Total Environ 473-474:659–666

Stocker T, Qin D, Plattner G, Tignor M, Allen S, Boschung J, Nauels A, Xia Y, Bex B, Midgley B (2013) IPCC, 2013: climate change 2013: the physical science basis. Contribution of working group I to the fifth assessment report of the intergovernmental panel on climate change

Tiwari S, Singh A (2013) Variability of aerosol parameters derived from ground and satellite measurements over Varanasi located in the Indo-Gangetic Basin. Aerosol Air Qual Res 13:627–638

Tiwari S, Srivastava AK, Singh AK, Singh S (2015) Identification of aerosol types over Indo-Gangetic Basin: implications to optical properties and associated radiative forcing. Environ Sci Pollut Res 22:12246–12260

Tiwari S, Tiwari S, Hopke P, Attri S, Soni V, Singh AK (2016) Variability in optical properties of atmospheric aerosols and their frequency distribution over a mega city "New Delhi," India. Environ Sci Pollut Res 23:8781–8793

Tripathee L, Kang S, Rupakheti D, Zhang Q, Huang J, Sillanpää M (2016) Water-soluble ionic composition of aerosols at urban location in the foothills of Himalaya, Pokhara Valley, Nepal. Atmosphere 7:1–13

Tripathi S, Dey S, Chandel A, Srivastava S, Singh RP, Holben B (2005) Comparison of MODIS and AERONET derived aerosol optical depth over the Ganga Basin, India. Ann Geophys 23:1093–1101

Wan X, Kang S, Li Q, Rupakheti D, Zhang Q, Guo J, Chen P, Tripathee L, Rupakheti M, Panday AK, Wang W, Kawamura K, Gao S, Wu G, Cong Z (2017) Organic molecular tracers in the atmospheric aerosols from Lumbini, Nepal, in the northern Indo-Gangetic Plain: influence of biomass burning. Atmos Chem Phys 17:8867–8885

Wang S, Fang L, Gu X, Yu T, Gao J (2011) Comparison of aerosol optical properties from Beijing and Kanpur. Atmos Environ 45:7406–7414

Xiao ZY, Jiang H, Song XD (2017) Aerosol optical thickness over Pearl River Delta region, China. Int J Remote Sens 38:258–272

Xie Y, Zhang Y, Xiong X, Qu JJ, Che H (2011) Validation of MODIS aerosol optical depth product over China using CARSNET measurements. Atmos Environ 45:5970–5978

Xin J, Zhang Q, Wang L, Gong C, Wang Y, Liu Z, Gao W (2014) The empirical relationship between the $PM_{2.5}$ concentration and aerosol optical depth over the background of North China from 2009 to 2011. Atmos Res 138:179–188

Xu C, Ma YM, Panday A, Cong ZY, Yang K, Zhu ZK, Wang JM, Amatya PM, Zhao L (2014) Similarities and differences of aerosol optical properties between southern and northern sides of the Himalayas. Atmos Chem Phys 14:3133–3149